PHYSICAL REVIEW VOLUME 188, NUMBER 2 10 DECEMBER 1969

# Paramagnetic Resonance of $Ho^{3+}$ in a Trigonal Site in $SrF_2$†

U. Ranon*‡
*McDonnell Douglas Astronautics Company, Santa Monica, California 90406*

AND

Kenneth Lee*
*IBM Research Laboratory, San Jose, California 95114*

(Received 26 June 1969; revised manuscript received 11 September 1969)

A paramagnetic-resonance spectrum of $Ho^{3+}$ in a trigonal site in $SrF_2$ was observed. The spectrum is characteristic of a non-Kramers ion, and the asymmetric line shape indicates that the non-Kramers ground doublet requires low-symmetry strain distortions to split the doublet and observe paramagnetic-resonance transitions of the magnetic dipole type. The spectrum is interpreted in terms of a standard spin Hamiltonian for a non-Kramers doublet with the parameters $g_{\parallel}=18.2\pm0.1$, $\Delta_0=0.033\pm0.001$ cm$^{-1}$, $|A|=0.397\pm0.005$ cm$^{-1}$. The possibility of observing paraelectric resonance in this site, which lacks inversion symmetry, was investigated. A discussion of various possible eigenfunctions, transitions, and line shapes in crystal fields of threefold and fourfold symmetry is given.

## I. INTRODUCTION

The electron-paramagnetic-resonance (EPR) properties of rare-earth ions with an even number of electrons (non-Kramers ions) are markedly different from those of odd-electron ions. For odd-electron ions all energy levels in a ligand field are at least doubly degenerate (Kramers theorem[1,2]), thus ensuring a first-order Zeeman effect in each of these levels. Although cases exist in which the eigenfunctions of a doublet are such that EPR transitions within it are not allowed, these are rare exceptions. Usually EPR transitions in odd-electron ions (Kramers ions) are allowed with the applied oscillatory magnetic field perpendicular to the external magnetic field.

In the case of non-Kramers ions, there will be degenerate levels in any ligand field which has a $C_n$ axis with $n>2$. But although degenerate, many of these levels will not have a first-order Zeeman effect. On the other hand, some of the levels will be singlets, even in cubic symmetry,[3] and in some cases accidental degeneracy occurs, such as, for example, when two close-lying singlets form an effective doublet.

Griffith[4] has shown that, for any isolated doublet of a non-Kramers ion, the magnetic splitting factor $g_z$ can be different from zero, but $g_x\equiv g_y\equiv 0$. Here $z$ is the principal axis of the $g$ tensor and is, in most cases, parallel to the principal symmetry axis at the paramagnetic site. Since $g_x$ and $g_y$ are, respectively, proportional to the matrix elements $\langle\psi_1|J_x|\psi_2\rangle$ and $\langle\psi_1|J_y|\psi_2\rangle$ between the two states of the doublet, Griffith's result indicates that, in non-Kramers doublets, EPR would be observed only with a component of rf magnetic field $H_\mu$ along the local symmetry axis and the dc magnetic field.

Since the degeneracy in non-Kramers ions is accidental, any non-Kramers doublet can be split by a crystal field perturbation of low enough symmetry. If the ion is located at a site which has inversion symmetry, all eigenfunctions of the ground configuration have the same parity so that nonvanishing matrix elements will exist only for operators with even powers of the crystal electric field. If, however, the site symmetry is noncentrosymmetric, the eigenfunctions will have both even- and odd-parity components so that matrix elements for odd powers of the electric field can exist. In particular, linear effects in the electric field may be observed and transitions between the Zeeman levels may be induced by the electric part of the rf field. These phenomena have been investigated and discussed by Williams[5] and by Culvahouse *et al.*[6,7] These papers also contain references to previous work on this subject. It was shown by these authors that in some cases the electric dipole EPR transitions may be several orders of magnitude more intense than the magnetic dipole transitions.

## II. $Ho^{3+}$ IN $SrF_2$

Strontium fluoride has the fluorite structure in which divalent strontium cations occupy alternate body centers of monovalent-fluoride-anion cubes. This is shown in Fig. 1(a). Trivalent rare-earth ions readily substitute for strontium ions in the fluorite lattice. Since charge neutrality is destroyed by the substitution of a trivalent ion for a divalent one, charge compensation is required. This may be achieved in various ways, depending on the crystal growth method and the com-

---

† A preliminary account of this work is presented in Bull. Am. Phys. Soc. **11**, 203 (1966).

* Part of this work done while the authors were with the Analytical Instrument Division, Varian Associates, Palo Alto, Calif.

‡ Varian Analytical Instrument Division Postdoctoral Fellow, 1964–1966.

[1] H. A. Kramers, Proc. Acad. Sci. Amsterdam **33**, 959 (1930).

[2] See, e.g., M. Tinkham, *Group Theory and Quantum Mechanics* (McGraw-Hill Book Co., Inc., New York, 1964), pp. 141–144.

[3] K. R. Lea, M. J. M. Leask, and W. P. Wolf, J. Phys. Chem. Solids **23**, 1381 (1962).

[4] J. S. Griffith, Phys. Rev. **132**, 316 (1963).

[5] F. I. B. Williams, Proc. Phys. Soc. (London) **91**, 111 (1967).

[6] J. W. Culvahouse, D. P. Schinke, and D. L. Foster, Phys. Rev. Letters **18**, 117 (1967).

[7] J. W. Culvahouse, L. Pfortmiller, and D. P. Schinke, J. Appl. Phys. **39**, 690 (1968).

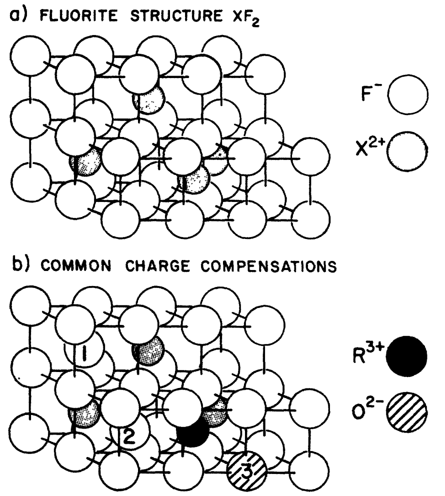

FIG. 1. Fluorite structure: (a) pure fluorite; (b) some charge compensations for trivalent rare-earth ions. For details see text.

pounds used as dopants. A few common charge compensation mechanisms in fluorites are shown schematically in Fig. 1(b). Any one of the positions 1–3 in the lattice can be a charge compensation site. 1 and 2 are interstitial $F^-$ ions. Site 1 creates an axial distortion of the ligand field at the rare-earth site along a $\langle 111 \rangle$ direction, giving the field a trigonal symmetry.[8,9] A fluorine anion on site 2 causes an axial distortion parallel to a cubic axis, thus creating a tetragonal symmetry.[8,9] Site 3 can accommodate a substitutional $O^{2-}$ ion, giving rise to a trigonal field that probably has a stronger axial component than case 1, because here the charge compensation is closer to the paramagnetic ion. Each of these three charge compensations causes the rare-earth site to be noncentrosymmetric. Less common are cases where the charge compensation occupies a more remote site giving rise to an orthorhombic field at the rare-earth site.[10,11] Frequently, the charge compensation is remote enough so that the cubic symmetry at the rare-earth site is preserved.

The cubic crystal field is characterized by two parameters $B_4$ and $B_6$, and the cubic field potential has the form[3]

$$V_c = B_4 O_4 + B_6 O_6 , \tag{1}$$

where $O_4 = O_4^0 + 5\ O_4^4$ and $O_6 = O_6^0 - 21\ O_6^4$; the $O_n^m$'s are the operator equivalents of Stevens.[12–14] Lea, Leask, and Wolf[3] expressed the potential (1) in terms of a parameter $x$, defined by $B_4/B_6 \propto x/(1-|x|)$, such that, for $0 \leq |x| \leq 1$, all values of $B_4/B_6$ are covered. These authors have computed and tabulated the energy levels and eigenfunctions for all $J \leq 8$ as a function of $x$. The sign of $x$ is determined from the point-charge model of the crystal field. Figure 2 shows the energy levels of $Ho^{3+}$ as a function of $x$ in the eightfold cubic coordination of the fluorite structure. Figure 3 shows the lowest three levels in more detail. The ground state is either a doublet $\Gamma_3^{(2)}$ or a triplet $\Gamma_5^{(2)}$. Attempts to observe EPR of $Ho^{3+}$ in a cubic site in the fluorites were unsuccessful,[15] so that probably $\Gamma_3^{(2)}$ is the ground state in the cubic site. In the present investigation no spectrum that could be attributed to $Ho^{3+}$ in cubic sites was observed.

Instead, the observed spectra are due to $Ho^{3+}$ ions in trigonal sites, in which the threefold axes are the cubic $\langle 111 \rangle$ orientations. There are four inequivalent sites of this type in the lattice. We have no direct evidence to show whether a charge compensation with an interstitial fluorine or a substitutional oxygen is responsible for the trigonal site symmetry [cases 1 and 3, respectively, in Fig. 1(b)]. But since the crystals were grown without the presence of oxygen in any form,[16] and because of similar experience with other impurities in

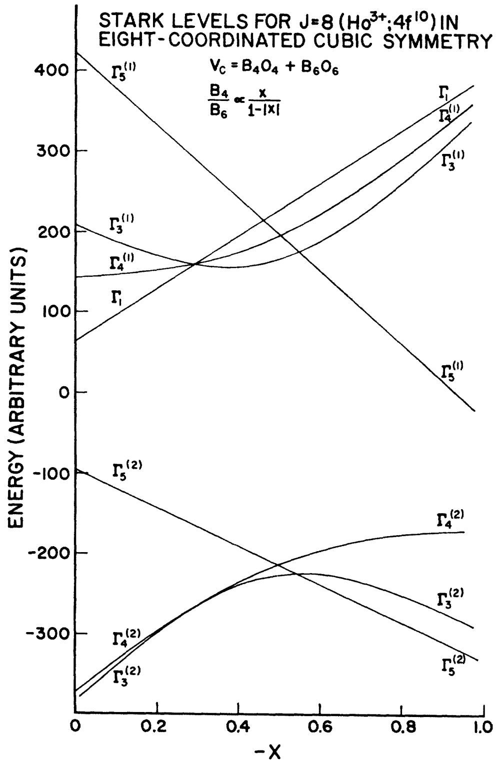

FIG. 2. Stark levels of the ground $J=8$ manifold of $Ho^{3+}$ in the fluorite structure (after Lea, Leask, and Wolf, Ref. 3).

---

[8] U. Ranon and A. Yaniv, Phys. Letters **9**, 17 (1964).

[9] M. J. Weber and R. W. Bierig, Phys. Rev. **134**, 1492 (1964).

[10] For example, S. D. McLaughlan, P. A. Forrester, and A. F. Fray, Phys. Rev. **146**, 344 (1966).

[11] E. Mahlab, W. Low, V. Volterra, and A. Yariv, Phys. Rev. **131**, 920 (1963).

[12] K. W. H. Stevens, Proc. Phys. Soc. (London) **A65**, 209 (1952).

[13] R. J. Elliott and K. W. H. Stevens, Proc. Roy. Soc. (London) **A215**, 437 (1952); **A218**, 553 (1953); **A219**, 387 (1953).

[14] M. T. Hutchings, in *Solid State Physics*, edited by F. Seitz and D. Turnbull (Academic Press Inc., New York, 1964), Vol. 16, p. 227.

[15] W. Hayes, G. D. Jones, and J. W. Twidell, Proc. Phys. Soc. (London) **81**, 371 (1963).

[16] R. A. Hargreaves (private communication); the crystals were obtained from Optovac, Inc.

the same host lattice,[8] the site symmetry is attributed to interstitial fluorine charge compensation of type 1 in Fig. (1b). Regardless of whether type-1 or type-3 charge compensation is operative, the site of the $Ho^{3+}$ ion is a noncentrosymmetric $C_{3v}$. In the next section the theoretical aspects of a non-Kramers ion in a noncentrosymmetric site are considered.

## III. THEORY

The total angular momentum $J$ of the $Ho^{3+}$ free ion in the ground state is $J=8$. This is the largest possible $J$ for an $f$ electronic shell in the ground state. Assuming Russell-Saunders coupling, the eigenfunctions of Stark levels in a crystal field with a $C_n$ axis ($n>2$) for integral $J$ in a general form are considered. The functions are linear combinations of $J_z$ eigenstates $|M\rangle$ and may be written in the form

$$\psi_i=\sum_k a_{ik}|M_k\rangle, \tag{2}$$

with $|M_k|\leq J$, $M_k-M_{k+1}=0$ (modulo $n$), and $\sum_k a_{ik}^2=1$. For a site with a principal threefold axis, the eigenfunctions fall into two categories:

$$\psi(\pm)=a|\pm8\rangle+b|\pm5\rangle+c|\pm2\rangle +d|\mp1\rangle+e|\mp4\rangle+f|\mp7\rangle \tag{3}$$

and

$$\phi=\alpha|6\rangle+\beta|3\rangle+\gamma|0\rangle+\delta|-3\rangle+\epsilon|-6\rangle. \tag{4}$$

The functions are written explicitly for $J=8$, but they will hold true for any integral $J$ by omitting the terms $|M_k\rangle$, for which $|M_k|>J$. The functions $\psi(\pm)$ can be associated with doublets, while the function $\phi$ is associated with singlets.

When a cubic field potential is expressed in a trigonal coordinate system with the $z$ axis along a cube body diagonal $\langle 111\rangle$, the $\Gamma_5$ triplet is composed of functions of the form $[\psi(\pm),\phi]$ and the $\Gamma_3$ doublet is composed of $\psi(\pm)$ functions. Lowering of the local symmetry will first split the triplet into a $\psi(\pm)$ doublet and a $\phi$ singlet. If one assumes that the $C_{3v}$ crystal field at the $Ho^{3+}$ site is created from a perturbation of the cubic field by a trigonal distortion, then the three lowest Stark levels will be two doublets of the form (3) and a singlet of the form (4). In order to see what kind of microwave resonance transitions could be anticipated within or between such doublets and singlets, the spin Hamiltonian pertinent to this problem is now considered.

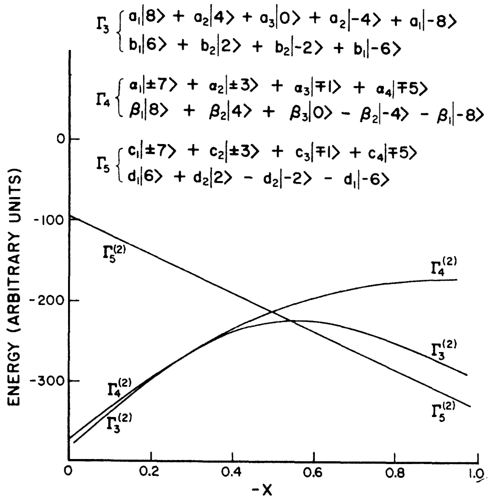

FIG. 3. Three lowest Stark levels of $Ho^{3+}$ in the cubic fluorite structure and their wave functions (after Lea, Leask, and Wolf, Ref. 3).

Williams[5] has shown that the general form of the spin Hamiltonian for a non-Kramers doublet (with effective spin $S=\frac{1}{2}$) and axial symmetry is

$$\mathcal{H}=g_{\parallel}\beta H_zS_z+AS_zI_z+\Delta_xS_x+\Delta_yS_y +P[I_z^2-\tfrac{1}{3}I(I+1)], \tag{5}$$

where the hyperfine term $AS_zI_z$ and the quadrupole term $P[I_z^2-\frac{1}{3}I(I+1)]$ have been included. Griffith[4] has demonstrated that $g_{\perp}\equiv0$ and, thus, there is only one Zeeman term. This is also the reason why no additional hyperfine terms are present. The two off-diagonal terms represent the effects of strain in the crystal. This can be due to two parts. First, random strains can arise from the misfit of the paramagnetic ion in its site and from the influence of a charge compensation when it is present. Further strain can be induced by an external electric field applied in the perpendicular plane. The effect of this field can be written[5]

$$\mathcal{H}_{\text{eff}}=G_{\perp}\beta(E_xS_x+E_yS_y), \tag{6}$$

where $G_{\perp}\neq0$ only in a noncentrosymmetric site. $G_{\perp}$ is a measure of the strain introduced by the external electric field. The spin Hamiltonian (5) can be solved rigorously because there are no off-diagonal elements in the nuclear spin $I$. A nuclear Zeeman term $g_N\beta_N\mathbf{H}\cdot\mathbf{I}$ could couple different nuclear states, but in the present case $g_N\beta_NH$ is of the order of $10^{-2}$ G and can be neglected. The eigenvalues of Eq. (5) are

$$E(\pm,m)=P[m^2-\tfrac{1}{3}I(I+1)] \pm\tfrac{1}{2}[(g\beta H_z+Am)^2+\Delta^2]^{1/2}, \tag{7}$$

where $\Delta=(\Delta_x^2+\Delta_y^2)^{1/2}$, $m$ is an eigenvalue of $I_z$, and $\pm$ are the two electronic states of the doublet. Because Eq. (5) is diagonal in $I$, only transitions with $\Delta m=0$ are allowed, so that

$$h\nu=[(g_{\parallel}\beta H_z+Am)^2+\Delta^2]^{1/2}, \tag{8}$$

where $\nu$ is the microwave frequency.

If this spin Hamiltonian is applied to the doublet $\psi(\pm)$ of the form (3), the resultant eigenfunctions are

$$\Phi(\pm)=N[\psi(\pm)\pm(|\Delta|/2h\nu)\psi(\mp)], \tag{9}$$

with $N=[1+\Delta^2/(2h\nu)^2]^{-1/2}$. Because $g_{\perp}\equiv0$, the only operator for magnetic dipole transitions is $\Delta\beta\mathbf{H}\cdot\mathbf{J}_z$. Thus the magnetic dipole transition intensity is propor-

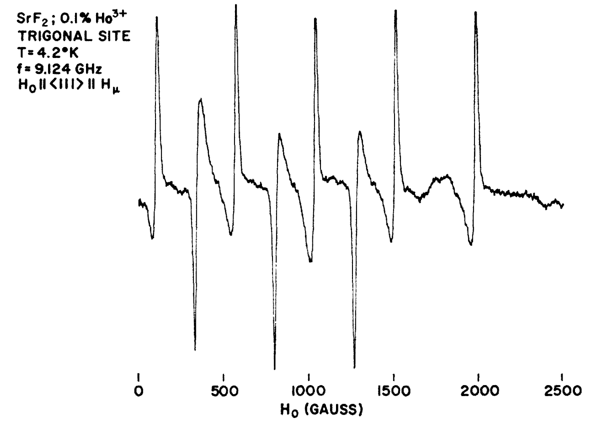

FIG. 4. First derivative of the absorption spectrum of SrF$_2$;Ho$^{3+}$ at $X$ band.

tional to

$$[g_{\parallel}^2\beta^2\Delta^2/4(h\nu)^2]H_{\mu,\parallel}^2, \tag{10}$$

where $\Delta \ll h\nu$, and $H_{\mu,\parallel}$ is the parallel component of the microwave magnetic field.

The electric dipole transition intensity is proportional to

$$\gamma_{\perp}^2\beta^2[1-\Delta^2/4(h\nu)^2]^2E^2 \quad (\Delta \ll h\nu). \tag{11}$$

$\gamma_{\perp}$ represents $G_{\perp}$, which is caused by the intracrystalline strain and has been calculated in a few cases.[5,7]

The spin Hamiltonian (5) was first used by Baker and Bleaney[17] in an investigation of non-Kramers ions in ethyl sulphates. In order to explain the asymmetric line shape observed in some cases,[17] they assumed that $\Delta$ is not single-valued, but rather has a distribution $P(\Delta^2/\Delta_0^2)$ centered about $\Delta_0$. If the distribution function is Gaussian, the density of states will be

$$\rho(\Delta^2) \propto \exp(-\Delta^2/\Delta_0^2)d(\Delta^2/\Delta_0^2). \tag{12}$$

Following Baker and Bleaney,[17] $H_z = H_0 - H'$, where $H_0$ satisfies the relation

$$h\nu = |g_{\parallel}\beta H_0 + Am|, \tag{13}$$

and is the position of a resonance line for $\Delta = 0$.

From Eqs. (13) and (8)

$$\Delta^2 = 2g_{\parallel}\beta H' h\nu \quad (\Delta \ll h\nu), \tag{14}$$

so that

$$d(\Delta^2) = 2g_{\parallel}\beta(h\nu)dH' \tag{15}$$

and

$$\rho(\Delta^2) \propto e^{-H'/H_0'}dH'. \tag{16}$$

Combining expression (10) and Eqs. (14) and (16), the magnetic dipole transition line shape is

$$f_H(H') \propto \tfrac{1}{2}(g_{\parallel}\beta H'/h\nu)e^{-H'/H_0'}. \tag{17}$$

The electric dipole transition line shape is

$$f_E(H') \propto (1 - g_{\parallel}\beta H'/2h\nu)^2 e^{-H'/H_0'}. \tag{18}$$

The intensity of a resonance line is then

$$I = f_H(H')(g_{\parallel}\beta H_{\mu,\parallel})^2 + f_E(H')(\gamma_{\perp}\beta E_{\mu,\perp})^2. \tag{19}$$

Since the absorption rises steeply from $H'=0$ to $H'=H_0'$ and drops slowly afterwards, the magnetic dipole line shape (17) is asymmetric. From Eqs. (8) and (13), it is seen that (i) when $Am > -|g_{\parallel}\beta H_0|$, then $H_0 > H_z$, and (ii) when $Am < -|g_{\parallel}\beta H_0|$, then $H_0 < H_z$. This means that $H'$ is measured in the direction of decreasing field in the first case, while in the second case it is measured in the direction of increasing field. Therefore the magnetic dipole absorption lines will show a sharp drop on the high-field side in case (i) and on the low-field side in case (ii). This is experimentally verified from Figs. 4–6, which show the derivative of the absorption and the transitions involved.

So far, a non-Kramers doublet of the form (3) has been discussed. In a trigonal field, such as that of $C_{3v}$ symmetry, this doublet transforms like the $E$ representation of the $C_{3v}$ group. Rather than have this doublet as a ground state, it is possible to have two close singlets of the form (4) as the lowest states. These singlets can belong to either one of the two one-dimensional representation $A_1$ and $A_2$ in $C_{3v}$. They can be considered as a split doublet, but now the zero-field splitting is a result of the over-all crystal field, and no strains are required to create this splitting. The $z$ component of the magnetic dipole operator transforms as $A_2$ in $C_{3v}$, and one has to consider three possibilities for the lowest doublet; (a) Both states are $A_1$; (b) both states are $A_2$; and (c) one state is $A_1$ and the other is $A_2$. In this symmetry $A_2 \times A_1 = A_2$, $A_2 \times A_2 = A_1$, $A_2 \times E = E$, so that in cases (a) and (b) the transitions are forbidden. Only in case (c) are transitions allowed. The functional form of the states [Eq. (4)] also suggests that transitions for $H_{\mu}$ parallel to the $z$ axis are allowed without requiring the admixture of the two states. If $\Delta_0$ is the splitting between the two singlets, the applied magnetic field $H$ in the $z$ direction will admix them by an amount $H/\Delta_0$. However, such an admixture is not necessary for

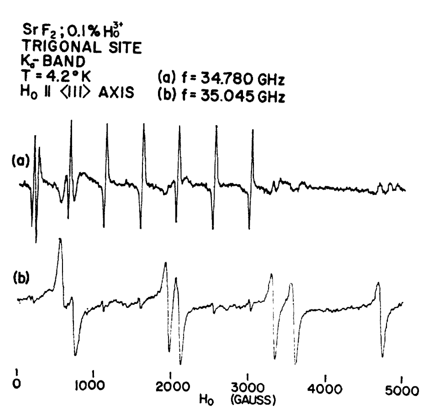

FIG. 5. First derivative of the magnetic dipole absorption lines at $K_a$ band for two different orientations of the external magnetic field $H_0$ relative to the microwave magnetic field.

---

[17] J. M. Baker and B. Bleaney, Proc. Roy. Soc. (London) **A245**, 156 (1958).

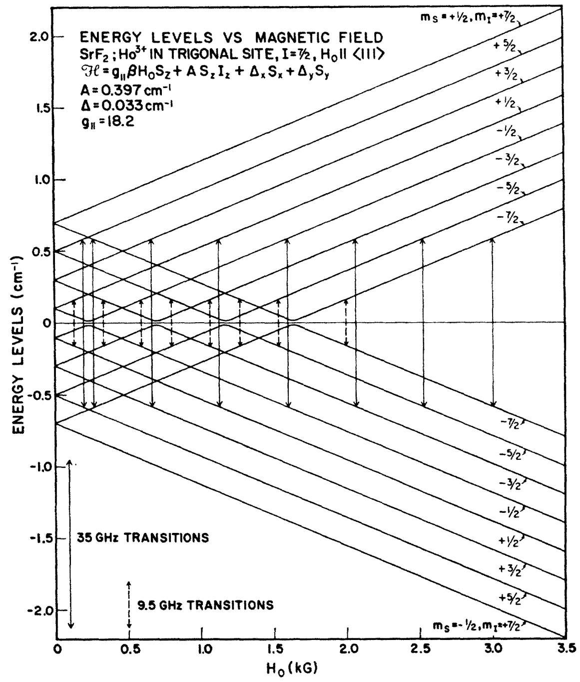

FIG. 6. Energy levels and transitions at $X$ band and $K_a$ band, as calculated from the experimental results.

the observation of EPR transitions. In this sense the spin Hamiltonian (5), using an effective spin representation, does not reflect a true physical picture of the states, since in this representation, assuming $\Delta \equiv \Delta_0$, the off-diagonal term $\Delta_0$ is the only one that connects the states and gives rise to a resonance. As pointed out by Culvahouse *et al.*[6] and by Mueller,[18] the spin Hamiltonian (5) is not invariant under a reflection in a plane perpendicular to the main symmetry axis. This is because $\Delta_x$ and $\Delta_y$, as well as $E_x$ and $E_y$, remain invariant under such reflection, while $S_x$ and $S_y$ change sign. In order to have an invariant spin Hamiltonian that describes the non-Kramers doublet with true angular-momentum operators, Mueller[17] proposed the use of a spin Hamiltonian with effective spin $S=1$.

Nothing has been said so far about the actual crystal field mechanism that will admix the states in a $\psi(\pm)$ doublet and cause their splitting. In order to obtain such a splitting, operators that have nonvanishing matrix elements between the two states $\psi(+)$ and $\psi(-)$ are required. Examination of these functions in (3) shows that operators $O_n{}^m$ with $m=1, 2, 4, 5, 7, \ldots$, may have such nonvanishing matrix elements.

The crystal field for a centrosymmetric site of threefold symmetry has the form

$$V' = b_2{}^0 O_2{}^0 + b_4{}^0 O_4{}^0 + b_4{}^3 O_4{}^3 + b_6{}^0 O_6{}^0 + b_6{}^3 O_6{}^3 + b_6{}^6 O_6{}^6, \tag{20}$$

where the coefficients $b_n{}^m$ are crystal field parameters. The addition of a noncentrosymmetric distortion, such as that due to one interstitial F$^-$ ion in the body center of a nearest cube along a body diagonal, adds to this potential a term of the form

$$V_A = \sum_n \alpha_n O_n{}^0, \tag{21}$$

where $\alpha_n = -r^n[\pi/(2n+1)]^{1/2}[1/2^n d^{n+1}]$. $r$ is the radius of the $4f$ electron distribution and $d$ is the F$^-$ rare-earth distance ($\frac{1}{2}$ the cube body diagonal). If the distortion is such that the paramagnetic ion is slightly displaced along an arbitrary direction $\zeta$ by an amount $\Delta\zeta$, the potential will change, to first approximation, by an amount[19]

$$\frac{\partial V}{\partial \zeta}\bigg|_{\zeta=0} \Delta\zeta, \tag{22}$$

where $V = V' + V_A$. In this case one can choose a coordinate $x$ in a plane perpendicular to $z$ such that $\zeta^2 = x^2 + z^2$. The distortion term (22) will then contain terms like $(\partial V/\partial x)\Delta x$ and $(\partial V/\partial z)\Delta z$; these, in turn, contain derivatives of the spherical harmonics contained in the $O_n{}^m$ operators. Now[20]

$$\begin{aligned} \frac{\partial}{\partial x} O_n{}^m &= a O_{n-1}{}^{m-1} + b O_{n-1}{}^{m+1} + c O_{n+1}{}^{m-1} + d O_{n+1}{}^{m+1}, \\ \frac{\partial}{\partial z} O_n{}^m &= a' O_{n+1}{}^m + b' O_{n-1}{}^m. \end{aligned} \tag{23}$$

From these expressions it is noted that $V'$ will contribute only odd terms in $n$ to $\partial V/\partial\zeta$. The matrix elements of these inside the $\psi(\pm)$ doublet vanish because of parity considerations. But the axial part $V_A$ will contribute both odd and even terms in $n$ to the distorted field. Since $V_A$ contains only $O_n{}^m$ terms with $m=0$, the distortion terms (22) will contain terms like $O_n{}^0$ and $O_n{}^1$. The operator $O_n{}^1$ with even $n$ is just the one that can have nonvanishing matrix elements between the two states of $\psi(\pm)$ and can cause the desired splitting. This is brought about by the part of the distortion perpendicular to the trigonal axis. A distortion parallel to the $z$ axis cannot split the levels.

## IV. EXPERIMENTS AND RESULTS

Experiments were carried out from 4.2 to 1.8°K with conventional reflection-type paramagnetic-resonance spectrometers at $X$ band ($\sim$10 GHz) and $K_a$ band ($\sim$35 GHz). For magnetic dipole transitions, the samples were mounted either on the bottom center of a TE$_{102}$ rectangular cavity (at $X$ band), or at $\frac{1}{2}R$ off center on the bottom of a cylindrical TE$_{011}$ cavity, where $R$ is the radius of the cylinder (at $K_a$ band). For electric dipole transitions, the sample was mounted on

---

[18] K. A. Mueller, Phys. Rev. **171**, 350 (1968).

[19] We are indebted to Dr. D. Schinke for suggesting this procedure.

[20] See, e.g., G. Goertzel and N. Tralli, *Some Mathematical Methods of Physics* (McGraw-Hill Book Co., Inc., New York, 1960).

the long axis of the rectangular cavity at $\frac{1}{4}\lambda$ from the bottom.

The isotope $^{165}$Ho is 100% abundant and has a nuclear spin $I=\frac{7}{2}$. Therefore, an eight-line hyperfine spectrum is expected.

The measurements of the electric versus magnetic dipole transitions show that the magnetic dipole transitions are at least two orders of magnitude more intense than the electric dipole transitions.

Figure 4 shows the derivative of the $X$-band magnetic dipole absorption with both the external magnetic field $H_0$ and the microwave magnetic field $H_\mu$ along a trigonal $z$ axis. The asymmetric line shape that is characteristic of a non-Kramers doublet of type (3) is clearly seen in this figure. Careful measurements between 4.2 and 1.8°K were carried out in order to see whether any change occurs in the line shape, as might be expected if dynamical effects were responsible for the line shape. No observable change was found.

The $K_a$ band spectrum is shown in Fig. 5. Here experiments were done at two different orientations of the microwave field $H_\mu$ relative to the external field $H_0$. In Fig. 5(a), the spectrum was taken with the microwave field $H_\mu$ parallel to the external field $H_0$ and a $\langle 111\rangle$ axis. In this figure, there are several groups of weak lines; one group is at 3500 and another at 4800 G. Other groups are partially covered by the strong lines. The weak lines belong to the three trigonal sites whose principal axes are not parallel to the field $H_0$. In a cube, the four $\langle 111\rangle$ directions are not orthogonal to each other, so that when $H_0$ and $H_\mu$ are parallel to one of them there is always a component of both fields along the remaining directions. In order to verify this, a spectrum was observed in which $H_\mu$ and $H_0$ were perpendicular to each other such that $H_0$ was along the $\langle 111\rangle$ axis, while $H_\mu$ was along $\langle 1,-1,0\rangle$. This is shown in Fig. 5(b). $H_\mu$ is now perpendicular to two of the trigonal axes and inclined at 35° to the other two. Therefore, a relatively strong signal should be observed from the two latter sites, corresponding to two of the three weak lines in each group of Fig. 5(a). This is clearly seen in Fig. 5(b).

Actually, if the crystal were perfectly oriented, only one line should be seen instead of each weak three-line group in Fig. 5(a), and each strong two-line group in Fig. 5(b). This is because the trigonal sites involved in each group are equivalent as far as the orientation of $H_0$ is concerned. A slight misorientation of $H_\mu$ is responsible for the weak lines in Fig. 5(b). These lines come from the $\langle 111\rangle$ site that is parallel to $H_0$, as can be seen by comparison with Fig. 5(a).

The lines from the sites not parallel to $H_0$ should be seen at a field for which $g=g_z\cos\theta$, where $\theta$ is the angle between the cube body diagonal involved and the field $H_0$. Since $\cos\theta=\frac{1}{3}$, the results give $g=6$. At $K_a$ band, this spectrum should then be centered around 4500 G. Since the hyperfine splitting parameter is $A/g\beta$ G, the effective hyperfine splitting will vary as $1/\cos\theta$. This explains the large splitting between the intense line pairs in Fig. 5(b) compared to that in Fig. 5(a). Figure 5(b) shows only four of the eight hyperfine transitions.

The parameters of the spin Hamiltonian (5) determined from these spectra are

$$g_{\shortparallel}=18.2\pm0.1\,,$$
$$\Delta_0=0.033\pm0.001\ \text{cm}^{-1}\,,$$
$$|A|=0.397\pm0.005\ \text{cm}^{-1}\,,$$

where $\Delta_0$ is the center value of the $\Delta$ distribution. From Eq. (8), and the discussion in Sec. III, it is seen that $\Delta_0$ can be determined from the accurate measurement of the frequency $\nu$, hyperfine splitting $A$, and the magnetic field. The position for $\Delta_0$ is that where the derivative of the absorption line passes through zero on its steep side.

In Fig. 6, the energy levels and the transitions at $X$ band and $K_a$ band, as calculated from the experimental results, are shown. From Figs. 4–6, it can be seen that the lines that have a sharp slope at the low-field side are indeed those for which $Am$ is negative, and has a value $|Am|>g\beta H$, as discussed in Sec. III.

## V. DISCUSSION

In discussing the experimental results, the ground-state eigenfunction is considered first. From the discussion in Sec. IV, one would anticipate a function of type (3) because of the asymmetric line shape. If, for a moment, it is assumed that a very strong axial distortion is operative in the crystal, then all states will be doublets with eigenfunctions $|\pm M\rangle$, with the exception of a $|0\rangle$ singlet. For each doublet, $g_z=2\lambda\langle M|J_z|M\rangle=2\lambda M$, where $\lambda=5/4$ is the Landé factor of Ho$^{3+}$. Since $g_z=20$ and $g_z=15$ for $M=8$ and $M=6$, respectively, and, in the present case, $g=18.2$, the actual eigenfunction must contain the $\pm8$ component and, therefore, it is indeed of the form (3). From the measured $g_{\shortparallel}$ and from (3), it can be calculated that $0.87\leq|a|\leq0.97$. Thus the eigenfunction of the non-Kramers doublet is strongly axial, and has the form (3) with $|a|\gg|b|$, $|c|$, $|d|$, $|e|$, $|f|$.

On the other hand, the observed very weak electric dipole transitions indicate that any noncentrosymmetric component in the trigonal field should be small, and, indeed, it is well known that, for Kramers ions in axial sites in fluorites, the axial distortion is relatively small and can be treated as a perturbation of the cubic field.[21]

From the tables of Lea, Leask, and Wolf,[3] it is found that $g$, for the transitions between the doublet components of the $\Gamma_5{}^{(2)}$ triplet in the cubic field, is about 9.5 over the entire range of $x$ for which $\Gamma_5{}^{(2)}$ is the ground state (see Fig. 3). Therefore, small deviations from the cubic symmetry could hardly explain the experimental $g=18.2$. Similar difficulties arise when one starts with

---

[21] H. R. Lewis and E. S. Sabisky, Phys. Rev. **130**, 1370 (1963).

a $\Gamma_3^{(2)}$ ground state. If the trigonal ground state is assumed to arise from an admixture between $\Gamma_3^{(2)}$ and $\Gamma_4^{(2)}$, which are close to each other for $|x|<0.55$ (Fig. 3), it is difficult to understand why transitions between other components of these levels are not seen.

A dynamical mechanism responsible for the distribution $\Delta$ seems to be ruled out by the measurements between 1.8 and 4.2°K. It has been shown above how a distribution $\Delta$ explains the intensity and the line shape of the EPR spectrum in a non-Kramers doublet of the form (3) in threefold symmetry. Transitions between levels of type (4), where the eigenfunctions belong to the different representations $A_1$ and $A_2$, will usually have symmetrical line shapes because distortions are not required for observation of EPR. Of course, distortions due to strain may admit the eigenstates of the two levels, but their effect on the transition probabilities will be only of second order, so that their effect on the line shape would be small. This has been verified, for example, in the experiments of Baker and Bleaney.[17] Other examples of the former case are trigonal spectra of $Pr^{3+}$ and $U^{4+}$ in $CaF_2$,[22] where the transitions are between levels of $\psi(\pm)$ doublets.

It is illuminating to discuss the case of non-Kramers ions in sites with fourfold symmetry. The same line of reasoning used previously can be applied to this case. Just as in the discussion in Sec. II, the possible combinations of $M$ states in a field of fourfold symmetry may be written

$$\xi=a|8\rangle+b|4\rangle+c|0\rangle+d|-4\rangle+e|-8\rangle, \tag{24}$$

$$\eta(\pm)=\alpha|\pm7\rangle+\beta|\pm3\rangle+\gamma|\mp1\rangle+\delta|\mp5\rangle, \tag{25}$$

$$\zeta=a'|6\rangle+b'|2\rangle+c'|-2\rangle+d'|-6\rangle. \tag{26}$$

The behavior of a doublet $\eta(\pm)$ is similar to the previous $\psi(\pm)$ in that it requires distortions to admix the two states in order to observe resonance. The other two functions are each similar to the previous function $\phi$ in (4). Based on the previous discussion, and on a group-theoretical analysis of the magnetic dipole selection rules for transitions between singlets in $C_4$ or $S_4$ symmetry, asymmetric lines would be anticipated for $\eta(\pm)$ doublets and symmetric lines for transitions between singlets of type $\xi$ or of type $\zeta$.

Thus, for example, the spectrum reported here is very similar in appearance to the one observed by Kirton[23] for $Ho^{3+}$ in $CaWO_4$, where the site symmetry is $S_4$. In the latter case, the asymmetric line shape arising from an $\eta(\pm)$ doublet follows naturally from these arguments. The assumption[23] that a dynamical Jahn-Teller effect is responsible for the splitting of the doublet and for the asymmetric line shape in $CaWO_4$ is incorrect. Ham[24] has shown that a dynamical Jahn-Teller effect cannot lift degeneracies that are a consequence of site symmetry or of time-reversed conjugation. In $CaWO_4$, the ground state has time-reversal degeneracy[23] and belongs to a representation $E$ of the $S_4$ point group. Similarly, one can account for the symmetric line shape of $Tb^{3+}$ in $CaWO_4$ [25] and $CaF_2$,[25] where the transitions are between singlets of the form $\xi$.

Finally, it is interesting to make the following comment on the spectra of non-Kramers rare-earth ions in tetragonal sites in the fluorites. The charge compensation in this case is an interstitial $F^-$ ion in position 2 of Fig. 1. The field created by this extra charge at the rare-earth site has the same form as in the trigonal case, namely, Eq. (21). Now, if there is the same kind of distortion as in the trigonal case, so that the potential changes by the amount given in (23), an interesting result is obtained. The doublet functions $\eta(\pm)$, in a tetragonal field, require operators $O_n^m$ with $m=2$, 6, . . ., to admix and split the doublet. But it was seen that (22) will give rise only to $O_n^m$'s with $m\leq 1$. It would be possible to obtain $m=2$ from second-order terms in the variation of $V_A$, but these would be of very small magnitude. Therefore, an observation of asymmetric-line-shape spectra from $\eta(\pm)$ doublets in fluorites is excluded by these arguments. To our knowledge, all the spectra which have been reported to date on non-Kramers rare-earth ions in tetragonal sites in fluorites have symmetrical line shapes and are due only to singlets of the type (24) or (26).

## VI. SUMMARY

A discussion of the EPR properties of non-Kramers rare-earth ions and experimental results for trivalent Ho in a trigonal site in $SrF_2$ were presented. It was shown how eigenfunctions of the states involved in the resonance transitions are related to the line shapes and distortions in the crystal. The electric dipole transitions versus magnetic dipole transitions in noncentrosymmetric sites were also discussed.

## ACKNOWLEDGMENTS

We would like to acknowledge Dr. F. W. Addis for helpful discussions, and Dr. D. Hannon for critical comments concerning the manuscript. One of us (U.R.) would like to thank the staff of the Analytical Instrument Research Laboratory at Varian Associates, and especially Dr. J. S. Hyde, for their hospitality during the tenure of a postdoctoral fellowship.

---

[22] S. D. McLaughlan, Phys. Rev. **150**, 118 (1966).

[23] J. Kirton, Phys. Rev. **139**, A1930 (1965).

[24] F. S. Ham, Phys. Rev. **138**, A1727 (1965).

[25] P. A. Forrester and C. F. Hempstead, Phys. Rev. **126**, 923 (1962).

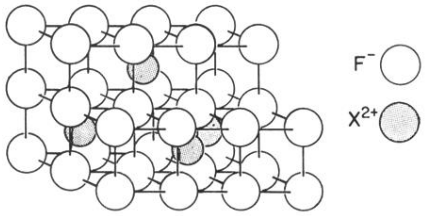

a) FLUORITE STRUCTURE $XF_2$

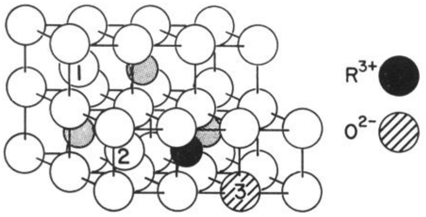

b) COMMON CHARGE COMPENSATIONS

FIG. 1. Fluorite structure: (a) pure fluorite; (b) some charge compensations for trivalent rare-earth ions. For details see text.